Ab initio studies of the $CoSi_2(100)/Si(100)$ interface

R. Stadler[1,2] and R. Podloucky[1]
[1]*Institute for Physical Chemistry of the University of Vienna, Liechtensteinstrasse 22A/1/3, A-1090 Vienna, Austria*
[2]*Physics and Astronomy Department, University College of London, Gower Street, London WC1 6BT, United Kingdom*
(Received 21 December 1999)

The Vienna *ab initio* simulation package based on ultrasoft pseudopotentials is applied for the calculation of (1×1) structures of the $CoSi_2(100)/Si(100)$ interface with sixfold, sevenfold, and eightfold coordinated Co positions at the interface. For the approximation to density functional theory the generalized gradient approximation is chosen. Three different formulations of interface energies are considered with and without strain energies. Relaxation of the atomic positions is very important for proper interface energies. All derived interface energies vary only within 0.06 eV depending on the geometry of the interface which suggests that kinetic effects are important for the epitaxial growth. A detailed analysis of local bonding effects is also provided. The analysis of the electronic structure focuses on interface localized states in particular for the eightfold coordinated type of interface showing directionally localized bonds and two bands of interface localized states with strong dispersion. The derived decay lengths of the electronic density towards Si show a similar dependence on Co coordination compared to that of previously studied (111) interfaces but are smaller in general. Schottky barriers for *p*-doped Si are calculated by two different approaches. Comparison to experiment yields that the eightfold coordinated interface is the only one reasonably close to the measured data.

I. INTRODUCTION

Extensive *ab initio* studies of the bulk[1] and surface properties[2,3] of $CoSi_2$ and the $CoSi_2(111)/Si(111)$ interface[4] were presented previously. $CoSi_2$ is of interest for the design of microelectronic devices[5] as pointed out in Refs. 1–4. Although as reviewed in Ref. 6, for the (111) orientation the conditions for epitaxial growth of $CoSi_2$ on Si are more favorable, there is increasing interest on the (100) interfaces due to their electronic transport properties. Concerning the actual structure of a (100) interface several differing structural models have been proposed, assuming additional dimerized Si layers,[7] (2×1) overstructures with defects[8] or strain-induced deformation.[9] The aim of the present work is to study the effects of the coordination of the atoms next to the interface on its energetics and electronic structure. For this purpose (1×1) structures resulting in a sixfold, sevenfold, and eightfold coordinated Co position were investigated.

II. COMPUTATIONAL ASPECTS

A. *Ab initio* method

For all the calculations the Vienna *ab initio* simulation package[10](VASP) was applied which was based on ultrasoft pseudopotentials according to Vanderbilt.[11,12] The numerical parameters and pseudopotentials were chosen in the same way as in Refs. 1,3,4. The set of **k** points was constructed according to a special **k**-point technique.[13–16] Choosing a $7\times7\times1$ grid resulted in 10 **k** points in the irreducible part of the Brillouin zone, the same setting as used for studying the $CoSi_2$ (100) surface.[3] All calculations were performed within the framework of density functional theory (DFT) utilizing the generalized gradient approximation (GGA) of Becke and Perdew[17] because of the excellent agreement with experimental data for bulk[1] and surface[3] properties of $CoSi_2$.

B. Geometrical aspects

Since Si crystallizes in the diamond structure and $CoSi_2$ in the CaF_2 structure, both systems have fcc sublattices. In the [100] direction, the stacking of the fcc Bravais lattice is AB. While in the diamond structure the two sublattices form a stacking sequence Si(A)-Si(A')-Si(B)-Si(B') in $CoSi_2$ a sequence Co(A)-Si(A)Si(A')-Co(B)-Si(B)Si(B') has to be built. The hyphens separate different layers and the primes distinguish different fcc sublattices of Si. The two Si sublattices form Si_2 layers taking turns with Co layers. For our calculations we used a supercell scheme for multilayers where a block of $CoSi_2$ alternates with a block of Si without any vacuum layers. By construction there are then two interfaces inside the three-dimensional unit cell. For correctly deriving interface properties, it is desirable to construct unit cells in which both interfaces are equal by symmetry. For the Si block this can be achieved by a number of layers restricted to $(4n+1)$, for $CoSi_2$ the situation is more difficult, since by cleaving the bulk material two different surfaces occur, one terminated by a Co layer the other by a Si_2-layer. Therefore, for building slabs with two symmetry equivalent interfaces a compromise has to be made, either by terminating the $CoSi_2$-block by a Si-layer with a single sublattice position on both sides [in this case the bulk-$CoSi_2$ stochiometry is preserved but the actual surface layer does not correspond to a bulk layer of (100) orientation] or by terminating it by Si_2 layers (in this case the $CoSi_2$ block does not have perfect bulk stochiometry).

Figure 1 shows views of the three different structural types of the $CoSi_2(100)/Si(100)$ interfaces under study. As in Ref. 4, Si positions of the $CoSi_2$ and Si block at the interface will be denoted by $Si_C(I)$ and Si(I), respectively. For the sake of simpler notations, $CoSi_2$ will be abbreviated by C. In general, the layers are numbered by (I–N) for the Nth layer away from the interface for both blocks. The $CoSi_2$ block of

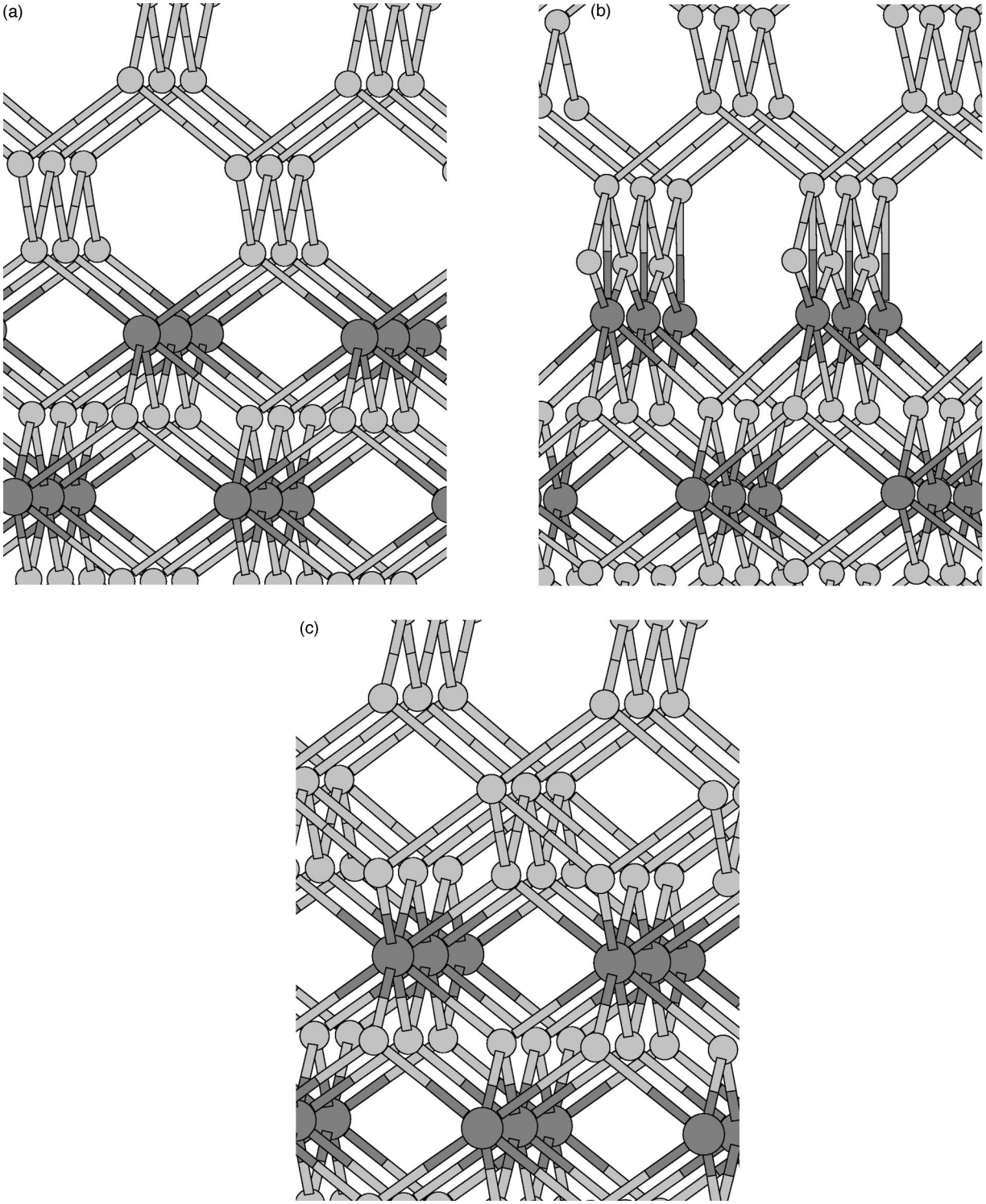

FIG. 1. Side view of the atomic arrangements for the structure types used to model the $CoSi_2(100)/Si(100)$ interface: (a) C6, (b) C7, (c) C8.

the first structure [Fig. 1(a)] is terminated by a Si layer built from a single fcc sublattice. Then Co(I-1) is undercoordinated surrounded by only six nearest neighbors and the $Si_C(I)$ sites continue the diamond structure of the Si block in an ideal way providing the remaining two of four nearest neighbors for Si(I) in its tedrahedral coordination. We denote this structure by C6 to account for the local coordination of the Co(I-1) sites.

Structure C7 [Fig. 1(b)] with sevenfold coordinated Co(I-1) can be formed from C6 by shifting the Si-block so that Si(I) has the same in-plane positions as Co(I-1), whereby Si(I) becomes now overcoordinated by five nearest neighbors. It must be noted, though, that in this case the distance Co(I-1)-Si(I) is larger than that of Co(I-1) to its two Si_C(I) and four Si_C(I-2) neighbors which will be discussed later in the section dealing with local bonding.

Structure C8 is the result of terminating $CoSi_2$ by a fully occupied Si_2 layer [Fig. 1(c)], because Co(I-1) atoms are now eightfold coordinated in the perfect $CoSi_2$-bulk environment. Si(I), however, is now strongly overcoordinated with six nearest neighbors. It should be noted, that due to the local environment defined by the Si(I-1) atoms there are now two different nonequivalent $Si_C(I)$ positions which we denote by $Si_C(I)A$ and $Si_C(I)B$.

For the actual calculations, 5 $CoSi_2$ bulk units and 13 Si layers have been stacked together for all structures resulting in total numbers of 28 atoms per unit cell for C6, C7, and 30 atoms for C8. The calculated lattice mismatch for $CoSi_2$ and Si is small, namely 1.9% with respect to the Si substrate, derived from the calculated equilibrium lattice constants of 5.350 Å for $CoSi_2$ and 5.454 Å for Si, respectively. If the Si spacing is chosen to be fixed, $CoSi_2$ has to be stretched in the plane defined by the interface orientation. Assuming standard elastic behavior, $CoSi_2$ contracts in the direction perpendicular to this plane. Accordingly, a contraction of -3.9% was derived from bulk calculations for which the planar lattice parameter for $CoSi_2$ was fixed to 5.454 Å and the lattice vector perpendicular to the (100) plane was varied until the energy was minimized. The strain energy for one bulk $CoSi_2$ unit in (100) orientation amounts to 0.018 eV.

Atomic layer distances at the unrelaxed interface were chosen to be 2.36 Å for the $Si_C(I)-Si(I)$ spacing for all stuctures. Ionic positions were allowed to relax for two Si layers and one $CoSi_2$ unit next to the interface.

III. RESULTS AND DISCUSSION

A. Interface energies

According to our studies of the (111) interface,[4] interface energies are derived by three different approaches: (1) from surface reference energies without the strain energy cost for $CoSi_2$, (2) same as (1) but strain added, and (3) from bulk cohesive energies. All interface energy values are defined per interface, the actually calculated results are divided by two because of two symmetric interfaces in the constructed unit cell.

Since—as discussed in the previous section—two identical surfaces of $CoSi_2$ cannot be formed just by cleaving the bulk phase in (100) orientation, the definition of interface energies is more complicated than for the (111) case.[4] To make the (100) termination of $CoSi_2$ symmetric some rebuilding of its surface layers have to be done which is different for C8 compared to C6, C7 interface structures.

For C6 and C7 structures, we define $E_{\mathrm{int}}^{(1)}$ by

$$E_{\mathrm{int}}^{(1)}(\mathrm{C6,C7}) = E_{\mathrm{bind}}(C/Si) + E_{\mathrm{surf}}^{0}(C) + E_{\mathrm{surf}}(Si) + E_{\mathrm{reb}}(C). \tag{1}$$

We consider three steps for the interface formations. First, free surfaces are formed by cleaving bulk $CoSi_2$ and Si resulting in surface energies of $E_{\mathrm{surf}}^{0}(\mathrm{C}) = 1.85$ eV and $E_{\mathrm{surf}}(\mathrm{Si}) = 2.05$ eV[3], correspondingly, for the unrelaxed surfaces. Superscript 0 denotes unstrained $CoSi_2$, whereas Si as the substrate is always unstrained according to Sec. II B. In a second step the energy contribution $E_{\mathrm{reb}}(\mathrm{C})$ has to be added accounting for rebuilding a cleaved bulk $CoSi_2$ slab for which one surface is originally terminated by an Si_2 layer and the other by a Co layer. This slab is rebuilt to a slab for which both surfaces are terminated now by Si layers belonging to one of the sublattices of Si. A value of $E_{\mathrm{reb}}(\mathrm{C}) = 0.25$ eV was calculated by directly comparing the cohesive energies of the two differently terminated $CoSi_2$ slabs,

$$E_{\mathrm{reb}}(C) = F_{\mathrm{surf}}(C, \text{Si term}) - F_{\mathrm{surf}}(\mathrm{C,cleav}) \tag{2}$$

in which the cohesive energies F are now calculated for the strained $CoSi_2$ block. The two different interfaces C6 and C7 are then formed by different stacking of the Si block on top of the Si-terminated $CoSi_2$ block according to Fig. 1 which results in two different interface energies.

Finally in a third step, rebuilt blocks of $CoSi_2$ and Si are put together forming a multilayer structure. The blocks now bind together with energy $E_{\mathrm{bind}}(\mathrm{C/Si})$ which we define by the difference of the cohesive energies F of the interface system and the two separated slabs within the same overall unit cell

$$E_{\mathrm{bind}}(\mathrm{C/Si}) = F_{\mathrm{int}}(\mathrm{C/Si}) - F_{\mathrm{surf}}(\mathrm{C,Si\ term}) - F_{\mathrm{surf}}(\mathrm{Si}). \tag{3}$$

[It should be noted that in Eq. (2) of Ref. 4 $F_{\mathrm{bind}}(\mathrm{C/Si})$ was erroneously used, it should be replaced by $F_{\mathrm{int}}(\mathrm{C/Si})$]. All surface like slabs entering Eqs. (2), (3) were created by either removing the Si block or the $CoSi_2$ block from the multilayer interface system. Because the unit cell is the same for all quantities—as argued in Ref. 4—the numerical accuracy is comparable. If—as was done for calculating E_{surf}—also the unrelaxed surfaces used for $F_{\mathrm{surf}}(\mathrm{C})$ and $F_{\mathrm{surf}}(\mathrm{Si})$ are chosen, then the interface energy should be independent of the state of relaxation of the free surfaces.

For the definition of the interface energy for the C8 structure, the expression

$$E_{\mathrm{int}}^{(1)}(\mathrm{C8}) = E_{\mathrm{bind}}(\mathrm{C/Si}) + E_{\mathrm{surf}}^{0}(\mathrm{C}) + E_{\mathrm{surf}}(\mathrm{Si}) + E_{\mathrm{form}}(\mathrm{Si_2}) + E_{\mathrm{ads}}(\mathrm{C,Si_2}) \tag{4}$$

has to be used since now $CoSi_2$ is terminated by Si_2 layers on both surfaces corresponding to filled sites of the Si sublattice. For the construction of this structure from cleaved $CoSi_2$, a Si_2 monolayer has to be formed and be adsorbed on the Co-terminated surface. Formation energy $E_{\mathrm{form}}(\mathrm{Si_2}) = 1.46$ eV accounts for the cost to form such a Si_2-monolayer from Si bulk being defined by

$$E_{\mathrm{form}}(\mathrm{Si_2}) = F_{\mathrm{mono}}(\mathrm{Si_2}) - 2F_{\mathrm{bulk}}(\mathrm{Si}). \tag{5}$$

An adsorption energy $E_{\mathrm{ads}}(\mathrm{C,Si_2}) = -1.80$ eV is gained by binding the Si_2 monolayer onto the Co-terminated surface as derived from

$$E_{\mathrm{ads}}(\mathrm{C,Si_2}) = F_{\mathrm{surf}}(\mathrm{C}) - F_{\mathrm{surf}}(\mathrm{C,cleav}) - F_{\mathrm{mono}}(\mathrm{Si_2}). \tag{6}$$

The definitions of interface energies by Eqs. (1) and (4) are independent of the strain energy of the $CoSi_2$ block. Therefore, it serves as a well-defined quantity independent on the number of actual layers involved in the calculation (assuming that the blocks are sufficiently thick so that the interfaces do not interact significantly). If the strain of n $CoSi_2$ trilayers is taken into account then the interface energy

TABLE I. Binding E_{bind} and three types of interface energies E_{int} as discussed in text for unrelaxed and relaxed geometries of $CoSi_2(100)/Si(100)$ interfaces. Unrelaxed data are denoted by (no). $E_{int}^{(1)}$: free unstrained surfaces as reference; $E_{int}^{(2)}$: sum of $E_{int}^{(1)}$ and total strain energy; $E_{int}^{(3)}$: derived from unstrained bulk cohesive energies. All energy values in eV.

	C6	C7	C8
E_{bind}(no)	−2.96	−2.81	−2.11
E_{bind}	−2.98	−2.94	−2.42
$E_{int}^{(1)}$(no)	1.18	1.33	1.45
$E_{int}^{(1)}$	1.16	1.20	1.14
$E_{int}^{(2)}$	1.25	1.29	1.23
$E_{int}^{(3)}$	1.28	1.33	1.26

$$E_{int}^{(2)} = E_{int}^{(1)} + nE_{strain}(C) \tag{7}$$

is derived (see Table I).

A third definition is made in terms of bulk cohesive energies by the differences of cohesive energies of the interface system, F_{int} and the corresponding bulk values F_{bulk},

$$E_{int}^{(3)} = F_{int}(C/Si) - F_{bulk}^{0}(C) - F_{bulk}(Si). \tag{8}$$

For the bulk reference of $CoSi_2$ the cohesive energy corresponding to 5 $CoSi_2$ units is taken into account, for Si bulk it corresponded to 13 Si atoms for structures C6 and C7, and 15 atoms for structure C8, respectively.

Table I presents interface and binding energies for the unrelaxed and relaxed $CoSi_2(100)/Si(100)$ ionic positions at the interface. The interface energies of C6, C7, and C8 after relaxing the atomic positions at the interface are rather similar within a range of 0.07 eV. However, this is not true for the binding energies, where structure C8 is energetically less favorable by 0.7 eV for unrelaxed and by 0.5 eV for relaxed ionic positions. The much smaller binding energy for C8 can be understood from the fact that for C8 the Co(I-1) sites already have their full coordination of 8 Si neighbors in the $CoSi_2$-block and therefore E_{bind} is built up only by Si-Si bonds.

The gain in binding energy is outweighed by the other contributions adding up to the interface energies, where for structures C6, C7 the energy $E_{reb}=0.25$ eV has to be invested to form the $CoSi_2$ block, in contrast to C8 for which energy is gained during the rebuilding process of the $CoSi_2$ block because the energy gain of negative $E_{ads}(C,Si_2)$ outweighs the energy loss of positive $E_{form}(Si_2)$ by 0.34 eV.

Apart from numerical accuracy concerns, $E_{int}^{(2)}$ and $E_{int}^{(3)}$ should be equal and show indeed the same trends. Structure type C8 is energetically the most favorable, followed by C6 and then C7, all energies within a small energy range of 0.07 eV. For structure C7 the 3 Si neighbors of the Co(I-1) sites at the interface are all located in the same plane perpendicular to the interface, which results in a distortion compared to $CoSi_2$ bulk. It seems that this distortion is responsible for the energetically less favorable position of C7. Very remarkably, structure C8 which becomes energetically most stable after relaxation of the ionic positions, is distinctly least favorable when unrelaxed. A detailed analysis of relaxation effects in terms of local bonding will be presented in the next section.

TABLE II. Interface energies $E_{int}^{(1)}$ in J/m^2 for $CoSi_2(100)/Si(100)$ and $CoSi_2(111)/Si(111)$. Rows refer to nearest-neighbor coordination of Co at the interface, columns compare results for the (100) interface structures (C) studied in the present work to the data for (111) interface types (A,B) given in Ref. 4. Total bulk like strain energy $nE_{strain}(C)$ for applied numbers n of $CoSi_2(100)$ and $CoSi_2(111)$ bulk layers is given in parentheses.

	100-C	111-A	111-B
sixfold	1.25 (0.10, $n=5$)		
sevenfold	1.29 (0.10, $n=5$)	0.56 (0.22, $n=5$)	0.61 (0.22, $n=5$)
eightfold	1.23 (0.10, $n=5$)	0.49 (0.27, $n=6$)	0.53 (0.27, $n=6$)

The interface energies $E_{int}^{(1)}$ in J/m^2 (Table II) for $CoSi_2(100)/Si(100)$ are more than twice as large as for $CoSi_2(111)/Si(111)$ derived from Ref. 4, but in both studies energetic differences between different interface structures are very small within a range of 0.06 J/m^2 (or 0.06 eV) for the studied (100) and 0.12 J/m^2 (or 0.10 eV) for (111) interfaces. Therefore, we conclude that independent from the crystallographic orientation of a $CoSi_2/Si$ interface the microscopic details of its structure are more likely to be determined by the kinetics of the growth process than by thermodynamical stability.

A critical number n_{crit} of strained $CoSi_2$ layers may be defined by

$$E_{crit} = E_{bind}(C/Si) + n_{crit}E_{strain}(C) \geqslant 0 \tag{9}$$

when the critical energy E_{crit} becomes positive. Then, the energy loss for straining all $CoSi_2$ units in the cell compensates the energy gain due to formation of chemical bonds at the interface. For structures C6, C7, and C8, this balance will be reached for $n_{crit} \sim 166$, 163 and 134 which corresponds to thicknesses of 432, 425, and 356 Å of strained $CoSi_2$. For $CoSi_2(111)/Si(111)$ interfaces the critical thicknesses are much smaller with values around 150 Å.[4] The reason for this can be found in the relation of strain energies per $CoSi_2$ bulk unit, which are twice as large for the (111) than for the (100) orientation, as well as in the binding energies which are about 50% larger for the (100) interfaces.

B. Interlayer spacing and local bonding

Table III presents the calculated interlayer distances after relaxation of ionic positions for all three interface types. The starting unrelaxed geometry is constructed from bulk distances which for $CoSi_2$ are calculated for the strained lattice.

Structure C6 reveals only very small small relaxation effects of interlayer spacings as reflected by the small relaxation energy of 0.02 eV. The chosen bulk distance between Si(I) and Si_C(I) layers remains unchanged. The only visible effect is a small reduction of the Co(I-1)–Si_C(I-2) distance which is a consequence of the undercoordination of Co(I-1) trying to shorten its distances to the remaining nearest neighbors. Because of this contraction in the $CoSi_2$ block spacings in the Si block are slightly expanded.

For structure C7, similar to C6 there is no change of the Si(I)–Si_C(I) spacing, but now for C7 a considerable 18% contraction of layer spacing Si_C(I)–Co(I-1) occurs. To acco-

TABLE III. Bulk and relaxed interlayer spacings in Å for the $CoSi_2(100)/Si(100)$ interfaces. First line: relaxed interlayer spacing next to center of Si block; last line: relaxed interlayer spacing next to center of $CoSi_2$ block. Si(*I*)-Si_C(I) spacing directly at the interface accentuated by horizontal lines. For C8, two different interface spacings due to SiC(I)A/SiC(I)B atoms (see text) occur.

Spacing	Bulk	C6	C7	C8
Si(I-2)-Si(I-1)	1.36	1.39	1.42	1.27
Si(I-1)-Si(I)	1.36	1.40	1.41	1.33
Si(I)-Si_C(I)		1.36	1.36	1.43/1.65
Si_C(I)-Co(I-1)	1.31	1.31	1.11	1.33/1.12
Co(I-1)-Si_C(I-2)	1.31	1.26	1.39	1.34

modate this contraction, the distances close to the Si bulk layer as well as between Co(I-1) and Si_C(I-2) are stretched. Since this is by far the most significant relaxation for structure C7, the major part of the relaxation energy of 0.13 eV must be attributed to it.

For structure C8 the relaxation energy reaches 0.31 eV. The interperation of relaxation effects is more complicated now because the two Si atoms of the Si_C(I) layer are not equivalent any more; they belong to two different fcc sublattices. Whereas one type of Si_C(I) layer atoms keeps its distance to Co(I-1) almost unchanged and only moderately increases its spacing to the Si(I) layer, the second type shows the same drastic Si_C(I)–Co(I-1) spacing contraction as found for C7 and also enlarges its distance to the Si(I) layer by 21%. Due to the overcoordination of Si(I) it gets pushed towards the Si block and therefore C8 is the only structure with Si bulk spacings contracted rather than expanded.

Substantial stretching of interface bond lengths between the two blocks was also measured by medium-energy ion scattering[18] and explained by frustrated dimers at the interface. Table IV summarizes bond lengths and coordinations of neighboring atoms up to a distance of 3.0 Å for atoms next to the interface. Discussing unrelaxed bond lengths, in contrast to the (111) orientation[4] for the (100) interfaces all eight Co-Si bonds within the $CoSi_2$ block have the same length but due to the strain forced by the lattice mismatch are stretched by 0.01 to 2.33 Å in comparison to the equilibrium bulk case. However, the six Si_1-Si_2 nearest neighbor bonds connecting the two different Si sublattices—which gave an important contribution to the cleavage energy of pure $CoSi_2$ (Ref. 3) and have an equilibrium length of 2.68 Å–are now split into four bonds in the Si_2 layer with a bond length of 2.73 Å and into two bonds perpendicular to the (100) plane with a bond length of 2.62 Å . The Si block is assumed to be in its bulk equilibrium with four Si-Si nearest neighbor bonds per unit cell each of the length of 2.36 Å .

For structures C6, C7 all four Si nearest neighbors of Si_C(I) in the plane are missing since they belong to the other sublattice which does not exist for the diamond structure of Si. Structure C7 is distinguished by Co(I-1)– Si(I) bonds which are absent for C6. These bonds seem to be strongly attractive since their length is reduced by 0.18 Å and only after relaxation their length becomes comparable to the bond lengths between Co(I-1) and its other six Si nearest neighbors. For C7, another important effect is the considerable reduction of lengths of bonds connecting Si_C(I) to Co(I-1) and Si_C(I-2). This effect is presumably a consequence of overcoordination of Si(I) which now has 5 nearest neighbors but it might also be related to the Si_C(I)–Si_C(I-2) bonds within the $CoSi_2$. Atoms in these two layers belong to the two different fcc sublattices. It should be noticed that for structures C6, C7 the Si_C(I) atom loses five out of six nearest Si neighbors by the cleavage and rebuilding process of the $CoSi_2$-block as described in Sec. III A.

TABLE IV. Number of symmetry equivalent neighbors *N* and bond lengths *d* in Å for atomic positions next to interface. Bond lengths given for relaxed geometries. Change due to relaxation Δ is given in parantheses: + elongation, − contraction.

	N	*d*(Δ)		
		C6	C7	C8
Si(I-1)	2(Si)	2.36(±0.0)	2.36(±0.0)	2.34(−0.02)
	2(Si)	2.38(+0.02)	2.39(+0.03)	2.36(±0.0)
	1(Si)			2.98 (+0.25)
Si(I)	2(Si)	2.36(±0.0)	2.37(+0.01)	2.34(−0.02)
	2(Si)	2.38(+0.02)	2.39(+0.03)	2.40(+0.04)
	2(Si)			2.54(+0.18)
	1(Co)		2.49(−0.18)	
Si_C(I)A	2(Co)	2.33(±0.0)	2.22(−0.11)	2.34(+0.01)
	2(Si)	2.36(±0.0)	2.37(+0.01)	2.40(+0.04)
	1(Si)	2.38(+0.02)	2.50(−0.12)	2.67(+0.05)
	4(Si)			2.74(+0.01)
Si_C(I)B	2(Co)			2.23(−0.10)
	2(Si)			2.54(+0.18)
	1(Si)			2.46(−0.16)
	4(Si)			2.74(+0.01)
	1(Si)			2.98(+0.25)
Co(I-1)	4(Si)	2.30(−0.03)	2.38(+0.05)	2.35(+0.02)
	2(Si)	2.33(±0.0)	2.22(−0.11)	2.23(−0.10)
	2(Si)			2.34(+0.01)
	1(Si)		2.49(−0.18)	

For C8, the Si_C(I) layer is still intact with positions of both Si sublattices of $CoSi_2$ filled. However, these sublattices are not symmetry equivalent anymore since one type of atoms in the Si_C(I) layer has now additional nearest neighbors in the Si(I-1) layer which is labeled by B to distinguish it from that of the other sublattice type marked by A. The symmetry breaking of Si_C(I)A and B atoms results in the major relaxation effects for C8. The strong enlargement of two Si_C(I)B–Si(I) bonds by 0.18 Å and one Si_C(I)B–Si(I-1) by 0.25 Å is certainly the driving relaxation force, because Si(I) atoms are overcoordinated with 6 nearest neighbors. For interface bonds belonging to Si_C(I)A, however, the stretching effect is much smaller with a maximum of 0.05 Å according to Table IV. Si_CB(I) atoms are also moving closer to Co(I-1) and Si_C(I-2) neighbors by 0.10 and 0.16 Å, respectively, which is certainly a consequence of the repulsive effects of the interface atoms of the Si block.

In conclusion, the strongest relaxations were derived for structure C8 for which repulsive effects between Si(I), Si(I-1), and Si_C(I) atoms are the main driving force. Considerable relaxations were also calculated for structure C7 for which Co(I-1)–Si(I) bonds are strongly reduced. Structure C6

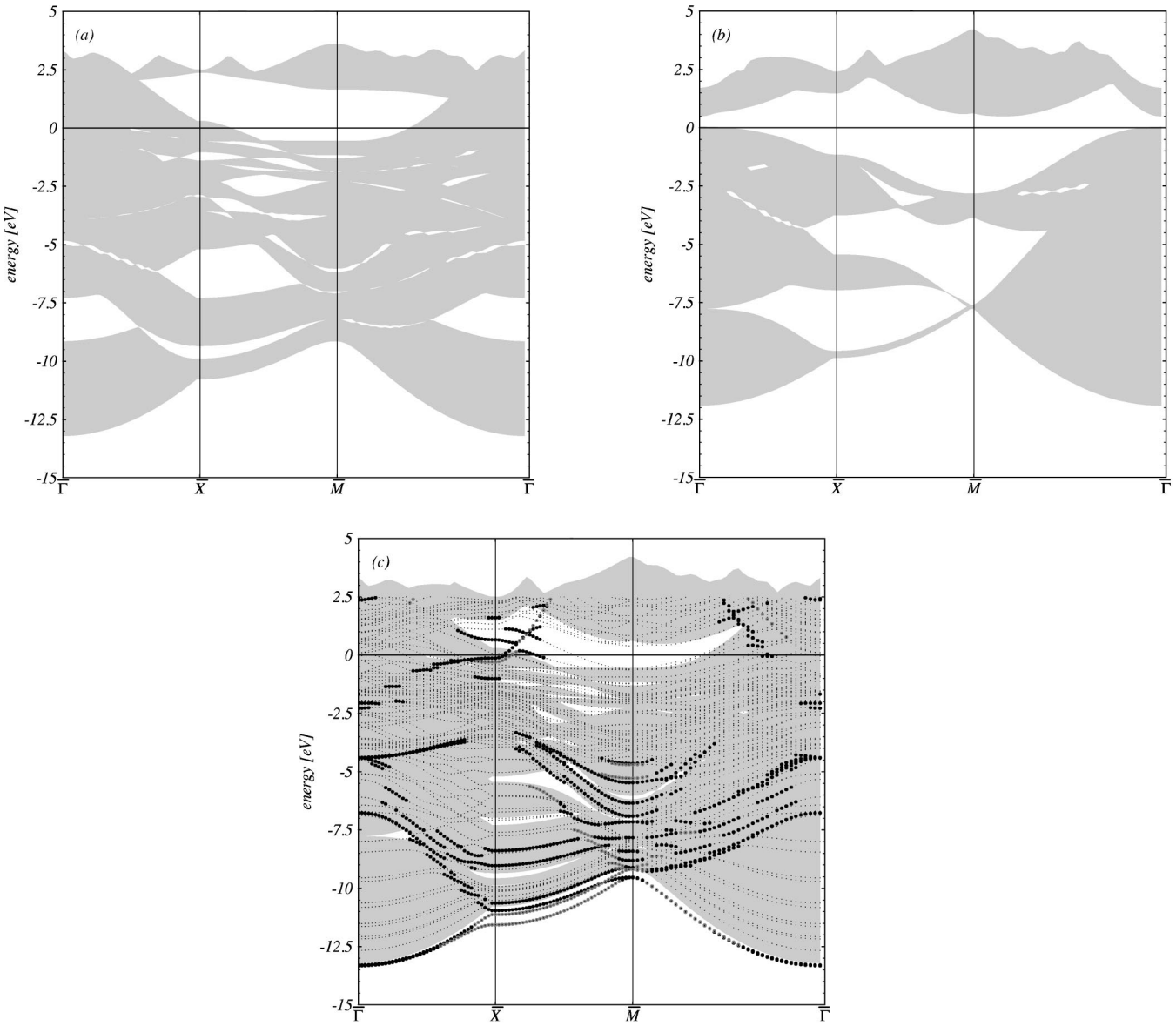

FIG. 2. Bulk bands projected along [100] orientation of $CoSi_2$ (a) and Si (b), and energy bands for the C8 interface type (c). Shaded area in (c): sum of projected bands of (a) and (b). Interface states localized at positions $Si_C(I)$ (Si interface site of $CoSi_2$ block): black circles; and Si(I) (Si interface site of Si block): grey circles. All other states: small dots. Further details for localization criterion see text. Fermi energy defined by zero of energy in all cases.

shows only minor relaxation effects. It should be noted that relaxation of ionic positions is very important for determining the atomic geometry and the interface energies as well.

C. Energy bands and interface states

Figures 2(a) and 2(b) show the projected bulk bandstructures of $CoSi_2$ and Si. The Fermi level in both cases [and also in the true interface results in Fig. 2(c)] is at zero energy, assuming that the noninteracting systems are in thermodynamical equilibrium. Further details are found in Ref. 4. For the (100) projection of $CoSi_2$ bands a large partial gap at -5 eV opens up around $\bar{X}$ whereas for the (111) case a similar but somewhat lower lying gap arises around $\bar{K}$. The principal gap is similar in shape and size in both cases. Overlaying the $CoSi_2$ and Si projected bands as done for the shaded area of Fig. 2(c) most of the gaps disappear. In particular in direction $\Delta\mathbf{k}_{XM} := \bar{X} - \bar{M}$ the two lowest, narrow Si bulk bands fit ideally into gaps of bulk $CoSi_2$. The lowest narrow band is nearly degenerate at $\bar{M}$ indicating localization in the z direction. As also discussed in Ref. 4 such a localized feature can be utilized to measure the potential shift along the interface normal due to the formation of an interface. This idea will also be exploited in the present study in Sec. III D.

In contrast to the (111) projections, for (100) the conduction band minimum of Si occurs now at two positions in $\mathbf{k}$ space, at $\mathbf{k}_{||} = \bar{\Gamma}$ and at $\approx 1/6 \times \bar{M} - \bar{\Gamma}$ in agreement with the bulk calculations of Mattheis and Hamann.[19] It should be noted that for Si the calculated gap of about 0.5 eV is, as usual, about two times smaller than the experimental value because standard density functional theory treats only the ground state properly and the Kohn-Sham eigenvalues have,

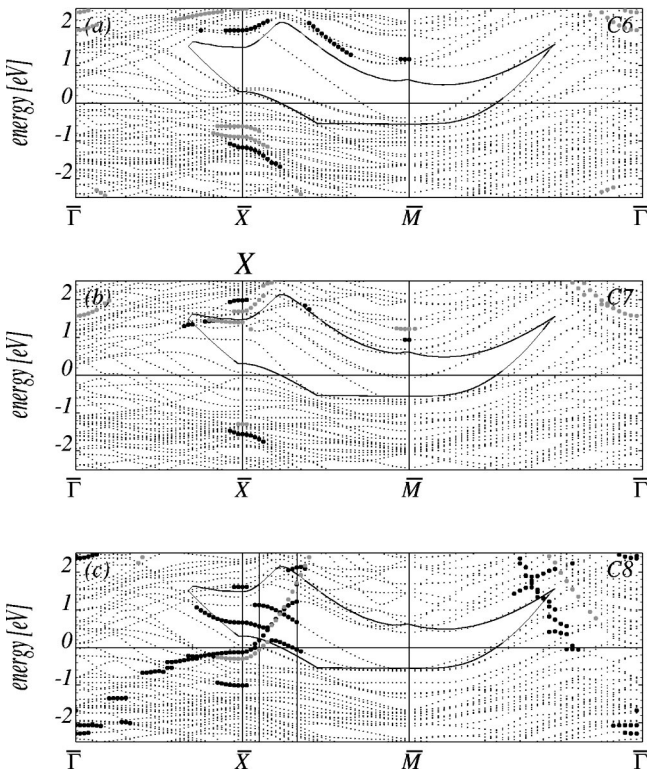

FIG. 3. Energy bands of structure C6 (a), C7 (b), and C8 (c) close to the principal gap. Further details see Fig. 2.

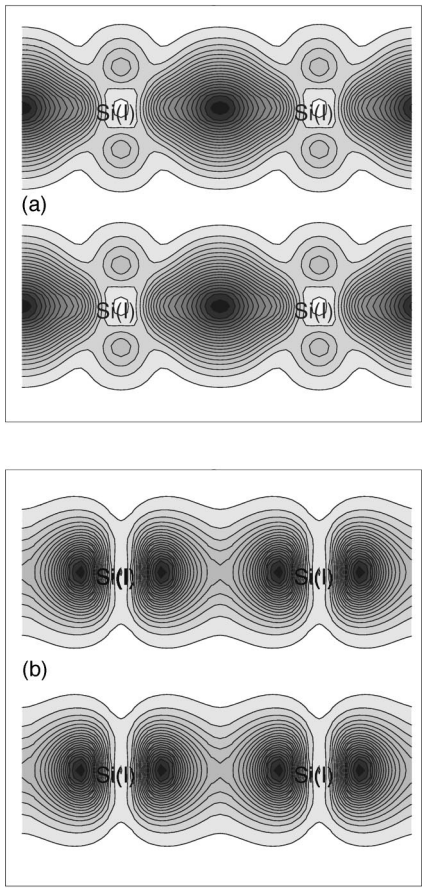

FIG. 4. Contour plots of charge density in the [001] plane through Si(I) positions for states at (a) $0.1\times\Delta\mathbf{k}_{XM}$ at 0.09 eV (band of strong dispersion) and (b) $0.325\times\Delta\mathbf{k}_{XM}$ at 1.18 eV (weak dispersion).

in principal, no physical meaning. Ballistic electron transmission through the interface for *n*-doped Si requires $CoSi_2$ conductions band states about 0.5 eV (which is approximately the experimental Schottky barrier) above the conduction band minimum of Si.[19,20] According to Figs. 2(a) and 2(b) suitable $CoSi_2$ states can be expected at $\bar{\Gamma}$. According to Ref. 19 three-dimensional bulk bands with proper symmetry are available there and the conditions for electronic transport are favorable as confirmed experimentally.[6]

Figure 2(c) shows the energy bands for interface structure C8 mapped onto the overlayed bulk projected bands. Only results for C8 are presented because they reveal the most rich and interesting interface features in comparison to C6 and C7. We define interface localized states when these states are localized more than 20% in spheres of radius 2.19 Å centered at Si(I) and Si_C(I) positions, and they are marked by gray and black dots, correspondingly. The same definition was used in the (111) interface study.[4] For C8, an abundancy of such interface localized bands occur in particular around $\bar{M}$, below the bulk projections and in the principal gap. Structure types C6 and C7 have much smaller number of interface localized states when compared to C8 with its overcoordinated Si atoms in the interface.

The states of the deepest well separated two or three bands [Fig. 2(c)] are well localized in the interface region within a range of about 5 Å as derived from planar averaged charge densities. For structure C6 no such localized low energy states occur, and for structure C7 one band of states localized at Si_C(I) appears lower in energy than the bulk projection in direction $\Delta\mathbf{k}_{XM}$.

Figure 3 focusses on the energy bands in the principal gap. A correlation of the number of interface bands in the gap and the local coordination of Si at the interface is visible, namely, the higher the coordination the more interface states or stronger localization occur. For interface type C6 only three interface bands with a moderate negative dispersion along $\Delta\mathbf{k}_{XM}$ are formed with a rather weak localization character. More bands (up to 8) arise for C7 with the same or somewhat stronger dispersion as C6.

For type C8, although the number of bands is about the same as for C7 new features occur: the lower states at $\bar{X}$ are distinctly more localized (black dots at lower energy, gray dots otherwise) and two spectacular bands of strong positive dispersion arise. The localized character of the corresponding band for $\Delta\mathbf{k}_{XM}\geqslant 0.3$eV is so strong that it maintains its localization even when going beyond the gap boundary and crossing through bulk conduction band states. This band reflects directional bonds at the interface region. Within a simple two-center tight-binding model the strong band dispersion must arise due to directionally localized bonds *parallel* to $\Delta\mathbf{k}_{XM}$ because then the Bloch factor $\exp(i\Delta\mathbf{k}\mathbf{R}_j)$ has the strongest variation. We restrict the interactions to hoppings between interface atoms Si(I) and atoms Si(I-1) or Si_C(I)B above or below the Si(I) layer, because there we find directionally localized bonds as demonstrated by Figs. 4–6. Furthermore, for a dispersive band it is necessary that the summation over *j* nearest neighbors does not cancel the hopping integrals which requires certain symmetry properties

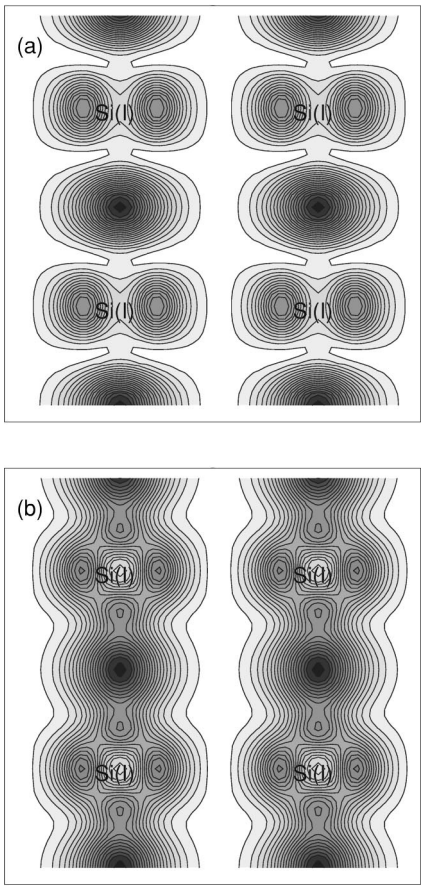

FIG. 5. Contour plots of charge density in the [001] plane through Si(I) positions for states at (a) $0.1\times\Delta\mathbf{k}_{XM}$ at 0.60 eV (band of weak dispersion) and (b) $0.325\times\Delta\mathbf{k}_{XM}$ at 1.75 eV (strong dispersion).

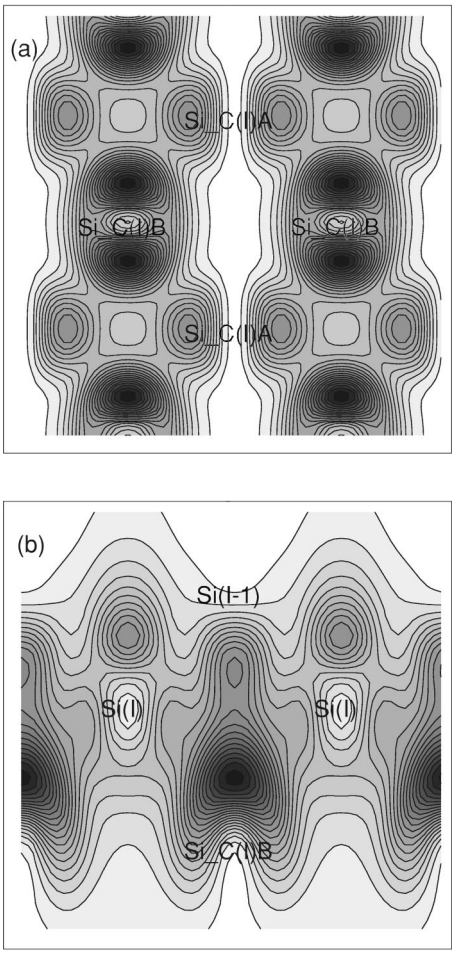

FIG. 6. Charge density contours for state at $0.325\times\Delta\mathbf{k}_{XM}$ at 1.75 eV in (a) a plane parallel to the interface through $Si_C(I)$ atoms and (b) a [100] plane through the atomic centers as shown.

from the orbitals involved. Inspection of Fig. 6(b) illustrates that atomic orbitals centered at Si(I), Si(I-1), and $Si_C(I)B$ must be symmetric with respect to rotations around the z-axis through the corresponding atomic centers. It should be noted that the distance Si(I)–Si(I) is a lattice vector, therefore the orientation of orbital lobes must be the same for both atoms. Orbitals of proper symmetry are p_z-like types for atoms $Si_C(I)B$ and Si(I-1), and s-like types for Si(I).

Parallel to chosen direction $\Delta\mathbf{k}_{XM}$ in reciprocal space for the band structure, the directions $\mathbf{R}_j$ in real space correspond to the projections of distance vector $\mathrm{Si}(I)-\mathrm{Si_C}(I)B$ or $\mathrm{Si}(I)-\mathrm{Si}(I-1)$ onto a (100) plane perpendicular to the [001] direction (or z direction). However, due to the geometrical construction there are two different interfaces in the unit cell, because one interface is rotated by 90° with respect to the other maintaining overall inversion symmetry. As a conseqence, for the fixed direction $\Delta\mathbf{k}_{XM}$ also directional bonds in direction $\mathrm{Si(I)}-Si_C(I)A$ are collected which are rotated by 90° compared to direction $\mathrm{Si(I)}-\mathrm{Si_C(I)B}$.

For the discussion of the charge density contours it has to be noted that because of the plane wave approach the contours do not show the correct nodal behavior in the vicinity of the atomic centers. This is not important anyway for discussing just the bonding features between the atoms.

For the two localized bands close to Fermi energy starting at X [Fig. 3(c)] which coincide at about $0.2\Delta\mathbf{k}_{XM}$ in Figs. 4,5 we present contour plots at $0.1\times\Delta\mathbf{k}_{XM}$ and $0.325\times\Delta\mathbf{k}_{XM}$ in the (100) plane cutting through Si(I) positions. The contours show bonds which are well localized in a particular direction, namely in the direction corresponding to the projection of $\mathrm{Si(I)}$-$Si_C(I)A$ in Fig. 4 and in the direction of projection of $\mathrm{Si(I)}$-$Si_C(I)B$ in Fig. 5 rotated by 90°. The positions of the Si_C atoms are also illustrated in Fig. 6(a).

Comparing the states of the two localized bands at $0.1\times\Delta\mathbf{k}_{XM}$, the state at lower energy [Fig. 4(a)] is of bonding character, the second state [Fig. 5(a)] belonging to a band of weak dispersion is rather antibonding in both main directions of the plane. At $0.325\times\Delta\mathbf{k}_{XM}$ the bonding character of both states changes in orientation corresponding to the changes in the steepness of their dispersion. Now, the antibonding state shown by Fig. 4(b) belongs to a band of weak dispersion whereas the bonding state in Fig. 5(b) is part of the strongly dispersing band. To complete the presentation of this state a cut through the Si_C layer is shown in Fig. 6(a) revealing directional bonding features of *p*-like character for both type of Si atoms. The layerlike localization of this particular state is strikingly depicted by Fig. 6(b) with distinctly p_z-like features above $Si_C(I)B$ and Si(I). The discussed mixture of rotated directed bonds is responsible for the interesting crossing behavior of bands at energies below 1 eV closer to X as shown in Fig. 3. It seems that the overcoordination of

Si of the C8 interface tries to keep the distribution of additional states, interface states, namely, away from both blocks of materials. This leads to the distinct bond localization as discussed, which is certainly correlated to the saturation of the dangling bonds of the Si(100) surface.

By summation over all states of the interface systems in the energy window defined by the valence band maximum and conduction band minimum of Si we derive the charge density ρ_{MIGS} comprising all the metal induced gap states. From the planar macroscopically[21] averaged ρ_{MIGS} we derive decay lengths λ which describe the decay of metallic $CoSi_2$ states into the Si block. The values of λ are 1.50, 1.33, and 2.78 Å for structures C6, C7, and C8, respectively. For $CoSi_2(111)/Si(111)$ interfaces values of 3.1 ± 0.1 for sevenfold and 4.4 ± 0.5 Å for eightfold coordinated structures were obtained. From these results it can be realized that independent from the interface orientation ρ_{MIGS} penetrates deeper into the Si block if Co(I-1) has its full bulk coordination but are decaying more rapidly if it is undercoordinated. More strikingly the decay lengths of ρ_{MIGS} are considerably smaller for the (100) orientation than in the (111) case. This finding indicates that the electrostatic potential at the interface is qualitatively different for both orientations which will be also demonstrated in the following section in terms of macroscopic averages of the electrostatic potential and Schottky barriers.

D. Schottky barriers

In the present study, Schottky barrier heights are derived by two different approaches: the first is based on the lineup of averages of electrostatic potentials,[21] and the second utilizes the energy shift of localized Si bulk states due to the presence of the interface. Both methods are outlined in detail in Ref. 4 where they have been used for $CoSi_2(111)/Si(111)$ interfaces.

Using the first approach the barrier height Φ_p for *p*-doped semiconductors can be written as[21]

$$\Phi_p^{\mathrm{av}} = \Delta E^{\mathrm{bulk}} + \Delta V \tag{10}$$

in which ΔE^{bulk} is derived from differences of Fermi energies and average electrostatic potentials in separate bulk calculations. For the present work on the (100) interface $\Delta E^{\mathrm{bulk}} = 3.51$ eV is obtained, which is slightly larger than the value of 3.26 eV for (111) interfaces.[4] The difference arises because we derived ΔE^{bulk} from bulk calculations for which $CoSi_2$ is strained according to the lattice mismatch and the amount of strain depends on interface orientation.

The potential lineup ΔV is the shift due to interface formation of the averaged electrostatic potentials $V_{\mathrm{av}}^{M,\mathrm{int}}$ and $V_{\mathrm{av}}^{S,\mathrm{int}}$ for the metal and semiconductor phase, accordingly and has to be derived from the actual interface calculations.

To evaluate ΔV now from electrostatic potentials a macroscopic averaging procedure[21] is used. To overcome the difficulties arising when the interface system consists of two bulk blocks with nonmatching lattices (in the present case, there are two different periods of *z*, namely, 5.241 Å for $CoSi_2$ and 5.454 Å for Si) we studied two different averaging procedures, as discussed in detail in Ref. 4. Procedure (1) which is a single average changing the period *a* abruptly when moving from the $CoSi_2$ block to Si; and procedure (2) which performs a rigorous twofold convolution.[21,4] In general for the averaging we used the sum of electronic and ionic potentials because—as pointed out by Baroni *et al.*[21]—Poisson's equation has to be solved for the total charge, electronic as well as ionic charge, in order to derive a physically meaningful electrostatic potential. Figure 7 shows the results for all three structure types.

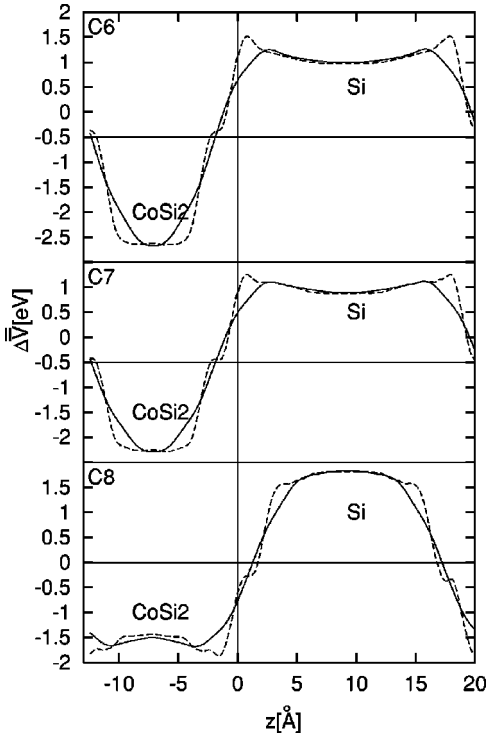

FIG. 7. Macroscopic average of the electrostatic potential according to procedures (1) (dashed line) and (2) (solid line) (see text) for interface types C6, C7, and C8 versus spacing z in direction [100]. Potential is shifted by a constant so that $\int \Delta V dz = 0$. Positive values of z: Si block, negative values: $CoSi_2$ block). Vertical lines: Co layers (solid) and Si layers (dashed).

The two averaging procedures yield rather similar results for the potential lineup. Differences occur in the interface region because of the small kinks generated by procedure (1). At the $CoSi_2$ block center procedures (1) and (2) differ by 0.06, 0.04, and 0.09 eV for C6, C7, and C8, respectively. For the (111) interfaces these differences were much larger, namely, up to about 0.2 eV[4] because the two procedures resulted in qualitatively different lineups in particular within the $CoSi_2$ block. The much better agreement of the macroscopic averages for (100) interfaces is due to the fact that the averaging periods in *z* direction are smaller for (100) than for the (111) orientation by about a factor of two. The general shape of potential lineups for C6, C7 is distinctly different from the lineup for C8 (Fig. 5): for C6, C7 a potential barrier arises at the interface because of charge pileup whereas for C8 a potential rise is found deeper inside the $CoSi_2$ block. Also the curvatures of lineups at the respective block centers are fundamentally different reflecting the distinctly different charge tranfers from one block to the other.

Similar to all-electron *ab initio* methods utilizing strongly localized core states, for our pseudopotential approach states strongly localized now in planes can serve as reference states for the change of potential. For this purpose the Si bulk like

TABLE V. Potential Lineups ΔV and p-type Schottky barrier heights Φ_p in eV. ΔV^2 and Φ_p^{av1}: derived from averaging procedure (1); ΔV^3 and Φ_p^{av2}: derived from averaging procedure (2); Φ_p^{loc}: derived from bulk localized Si 3s states; $\Phi_p^{QP,i}$: sum of Φ_p^i and quasiparticle corrections of 0.31 eV. Further details, see text. Experimental values 0.38–0.42 eV (Refs. [25,26]).

	C6	C7	C8
ΔV^1	−3.61	−3.14	−3.16
ΔV^2	−3.67	−3.18	−3.34
Φ_p^{av1}	−0.10	0.37	0.26
Φ_p^{av2}	−0.16	0.33	0.17
Φ_p^{loc}	−0.15	0.24	0.19
$\Phi_p^{QP,\mathrm{av1}}$	0.15	0.64	0.48
$\Phi_p^{QP,\mathrm{av2}}$	0.21	0.68	0.57
$\Phi_p^{QP,\mathrm{loc}}$	0.16	0.55	0.50

state at $\bar{M}$ at about -7.5 eV [Fig. 2(b)] is well suited. The overall agreement of Schottky barrier heights Φ_p derived from potential lineups and shifts by the three different approaches is satisfying (second block in Table V) yielding the same trend: a distinctly negative value for Φ_p is found for C6, it is positive and largest for C7 with the value for C8 positive and in between.

In order to compare calculated values of Φ_p to experimental results a correction has to be added[4] accounting for excitations which are not properly described within ground state density functional theory. Following the arguments of Godby *et al.*[22] an additive correction of 0.31 eV can be estimated if Si is the semiconductor of the interface system. Because of this crude estimation of quasiparticle effects the absolute values of the calculated Schottky barriers have some further uncertainties presumably in the order of 0.1–0.2 eV. But since the differences of Φ_p for the three different structures are much larger than the estimated uncertainty, we expect the calculated trend of barrrier height versus geometry to be meaningful. From ballistic-electron-emission spectroscopy (BEES) measurements of $CoSi_2(100)/Si(100)$ interfaces a value of $\Phi_p = 0.38 \pm 0.03$ eV (Refs. 23,24) was derived. An increase to $\Phi_p = 0.42 \pm 0.03$ eV (Ref. 24) was ascribed to defects. The quasiparticle corrected values $\Phi_p^{QP,i}$ in Table V reveal that only structure C8 is consistent to the experimental value, whereas $\Phi_p^{QP,i}$ is are far too small for C6 and far too large for C7.

Certain model assumptions[8] believe, that the interface structure is a sevenfold coordinated one, although the detailed atomistic geometry of the interfaces studied in the spectroscopy experiments is still unknown. Based on our extensive *ab initio* calculations of $CoSi_2(100)/Si(100)$ interfaces we conclude that the eightfold coordinated structure C8 is the most likely one to be found in the experiments because the calculated Φ_p is in reasonable agreement to experiment. One should also keep in mind that it was energetically the most favorable in terms of interface energies (although the energy differences were quite small).

IV. SUMMARY

We studied the energetical and electronic properties of the $CoSi_2(100)/Si(100)$ interface depending on the coordination of the atoms at the interface by means of state of the art *ab initio* calculations. Although the investigated sixfold, sevenfold, and eightfold coordinated interface types have rather different local bonding environments which is reflected in large relaxation effects the interface energies $E_{\mathrm{int}}^{(1)}$ after relaxation are only differing within 0.06 eV according to Table I (or 1.8% of the sum of the surface energies of $CoSi_2$ and Si). This is a strong indication that the growth process of the interface is governed by kinetic effects rather than by thermodynamical equilibrium. According to our calculations, structure C8 has the lowest interface energy as derived from two different approaches. In contrast to the $CoSi_2(111)/Si(111)$ interface, for the (100) orientation a large number of interface states can be found. A particular interesting result is found for the C8 structure with eightfold coordinated Co atoms which shows two bands of directional bonds in the interface region. A strongly dispersive band arises which keeps its localized interface character across the gap and also in the conduction band energy regime. From the comparison of the calculated Schottky barries to the experimental findings the C8 type interface seems to be the most preferable one.

ACKNOWLEDGMENTS

Work supported by the Austrian Science Foundation (FWF) under Project No. P10645-PHY. We thank also the Center for Computational Materials Science (CMS) for support. Thanks also to K. Reuter, T. Meyer, and H. v. Känel for very helpful discussions.

[1] R. Stadler, W. Wolf, R. Podloucky, G. Kresse, J. Furthmüller, and J. Hafner, Phys. Rev. B **54**, 1729 (1996).
[2] D. Vogtenhuber and R. Podloucky, Phys. Rev. B **55**, 10 805 (1997).
[3] R. Stadler, R. Podloucky, G. Kresse, and J. Hafner, Phys. Rev. B **57**, 4088 (1998).
[4] R. Stadler, D. Vogtenhuber, and R. Podloucky, Phys. Rev. B **60**, 17 112 (1999).
[5] R. Tung, Mater. Chem. Phys. **32**, 107 (1992).
[6] H. v. Känel, Mater. Sci. Rep. **8**, 193 (1992).
[7] D. Loretto, J. M. Gibson, and S. M. Yalisove, Phys. Rev. Lett. **63**, 298 (1989).
[8] C. W. T. Bulle-Lieuwma, Appl. Surf. Sci. **68**, 1 (1993).
[9] V. Buschmann, L. Fedina, M. Rodewald, and G. van Tendeloo, Philos. Mag. Lett. **77**, 147 (1998); J. Cryst. Growth **191**, 430 (1998).
[10] G. Kresse and J. Hafner, Phys. Rev. B **48**, 13 115 (1993); **49**, 14 251 (1994); **54**, 11 169 (1996); G. Kresse and J. Furthmüller, Comput. Mater. Sci. **6**, 15 (1996).
[11] D. Vanderbilt, Phys. Rev. B **41**, 7892 (1990).

[12] G. Kresse and J. Hafner, J. Phys.: Condens. Matter **6**, 8245 (1994).
[13] E. G. Moroni, G. Kresse, J. Furthmüller, and J. Hafner, Phys. Rev. B **56**, 15 629 (1997).
[14] S. G. Louie, S. Froyen, and M. L. Cohen, Phys. Rev. B **26**, 1738 (1982).
[15] H. J. Monkhorst and J. d. Pack, Phys. Rev. B **13**, 5188 (1976).
[16] M. Methfessel and A. T. Paxton, Phys. Rev. B **40**, 3616 (1989).
[17] A. D. Becke, Phys. Rev. A **38**, 3098 (1988); J. P. Perdew, Phys. Rev. B **33**, 8822 (1986).
[18] M. Copel and J. Falta, Phys. Rev. B **48**, 2783 (1993).
[19] L. F. Mattheis and D. R. Hamann, Phys. Rev. B **37**, 10 623 (1988).
[20] M. D. Stiles and D. R. Hamann, J. Vac. Sci. Technol. B **9**, 2394 (1991).
[21] A. Baldereschi, S. Baroni, and R. Resta, Phys. Rev. Lett. **61**, 734 (1988); S. Baroni, R. Resta, A. Baldereschi, and M. Peressi, in *Spectroscopy of Semiconductor Microstructures*, edited by G. Fasol, A. Fasolino, and P. Luigi, Vol. 206 of *NATO Advanced Studies Institute Series B. Physics* (Plenum, New York, 1989), p. 251.
[22] R.W. Godby, L.J. Sham, and M. Schlüter, Phys. Rev. Lett. **65**, 2083 (1990).
[23] H. Sirringhaus, T. Meyer, E. Y. Lee, and H. v. Känel, Phys. Rev. B **53**, 15 944 (1996).
[24] T. Meyer (private communication).